

Development of a High Strength Mill Spindle and Its Strength Evaluation*



Noriaki Inoue
Staff Assistant
Manager, Equipment
Technology Sec.,
Mizushima Works



Sadanori Nakano
Equipment Technology
Sec., Mizushima
Works



Noboru Kawauti
Equipment Technology
Sec., Mizushima
Works



Kazuaki Hamada
Staff Assistant
Manager, Equipment
Technology Sec.,
Mizushima Works



Tadashi Naito
Staff Manager,
Equipment Technology
Sec., Mizushima
Works

1 Introduction

The Slipper-metal-type mill drive spindle (SJ) has until recently seen no remarkable technical progress since the introduction of rolling mills into Japan. In the mean time, there has been a noticeable trend toward a rise in rolling torque in hot rolling mills and others mainly by the adoption of special techniques such as controlled rolling and high reduction both for controlling the mechanical properties of rolling materials, with the former especially for saving energy in reheating furnaces. Further, there has been a growing increase in

Synopsis:

No conspicuous progress has been made in spindles for rolling mill drives, and rolling torque loaded to the spindles has been greatly increased in recent years on account of very severe operating conditions. As a result, a lot of spindle yokes have cracked at the slipper metal groove and the trouble has caused serious damage to production.

In our research, the stress analysis of the spindle head and roll coupling was made, and stress concentration of the spindle yoke became clear, and through the analysis, a new type spindle which could reduce stress concentration was designed. It was confirmed that by the brittle lacquer coating test and stress measurement the new type spindle had double strength than that of the original. An experimental equation for estimating maximum stress loaded to the spindle was conducted and a diagram which showed the strength balance of spindle yoke and roll coupling was made out.

peak torque when rolling materials first comes in contact to work rolls, resulting in a sharp rise in torque amplification factor (TAF)¹⁾ (see Fig. 1).

Consequently, downtime due to insufficient strength of the mill drive system has increased. Fractured SJ requires a great deal of time to repair, involving not only repair costs but also loss of production opportunity, thereby inflicting a heavy damage.

In this paper, incidents of fractured SJ due to increased rolling torque, which have occurred frequently in recent years, are taken up as a problem. The SJ, not essentially improved in the past, is now examined for possible strength improvement measures and strength evaluation methods, mainly by use of stress analysis. This paper describes problems with the conventional SJ, and discusses strength property evaluation, the concept of a new type of SJ, a strength property evaluation experiment, derivation of experimental equations for maximum stress in the spindle yoke and roll coupling, and the strength balance-sheet of the spindle yoke and roll coupling. In addition, the paper reviews the superiority in strength of the new SJ and

* Originally published in *Kawasaki Steel Giho* 16(1984)3 pp. 221-231

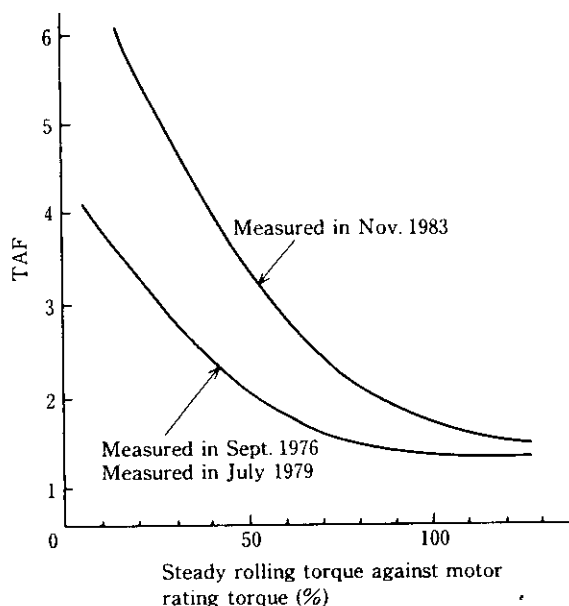


Fig. 1 Increase of torque amplification factor (TAF) at hot strip finishing mill

presents a strength evaluation.

2 Characteristics of SJ Fractures and Line of Investigation

Upon investigation of the surface of a fractured SJ, a fatigue crack as shown in Fig. 2 is observed at the corner of the slipper metal groove. This fatigue crack is under 10 mm in radius for a SJ with an outside diameter of 1 000 mm. Even SJ in use, which has not yet developed fracture, frequently shows cracks at the same corner as shown in Fig. 2, when subjected to liquid penetrant or magnaflux inspections.

On the other hand, no fracture or crack has ever occurred to roll coupling. This fact suggests an imbalance in strength between the spindle yoke and the roll

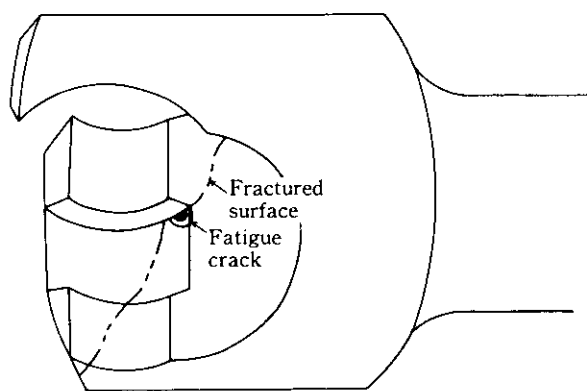


Fig. 2 Example of fractured SJ

coupling of SJ.

From the above, the following points are inferred:

- (1) Stress and stress concentration at the slipper metal groove of the spindle yoke have not yet been clarified, only known to be far beyond forecast.
- (2) The conventional strength calculation method²⁾ for the spindle yoke does not consider the stress concentration at the slipper metal groove and is suspected of over-estimating the strength of the spindle yoke.
- (3) It is suspected that the existing method of strength calculation for the roll coupling is not established, causing underestimation of its strength, further leading to the possibility that operating mill has been equipped with a roll coupling of too high a strength.

It is necessary, therefore, to undertake the following tasks, from the viewpoint of equipment technology, in order to improve the strength reliability of SJ and meet the need for high torque rolling:

- (1) To clarify the nature and cause of stress concentration at the slipper metal groove of the spindle yoke, and, on this basis, develop SJ which is free from stress concentration.
- (2) To establish a strength calculation method for the spindle yoke and roll coupling, and enhance the accuracy of strength evaluation.
- (3) To achieve a strength balance between the spindle yoke and roll coupling, and thereby increase the strength of the entire drive system.
- (4) For the purpose of item (3) above, to devise a strength balance sheet that mill easily give the strength relationship between the spindle yoke and the roll coupling.

In carrying out this study, it was necessary to make quantitative evaluations by such means as material mechanics, the finite element method, brittle lacquer coating tests, and stress measurement tests, and to ensure the high reliability of conclusions. It was also necessary to consider that the above examination concerns problems common to all SJs and to express the results of the examination in dimensionless expressions obtained by dividing the respective dimensional particulars by the outside diameter, thereby obtaining findings with universal validity.

3 Strength of the Spindle Yoke

3.1 Stress Analysis by the Finite Element Method

Since it was predicted that the stress concentration at the corner of the slipper metal groove would be high as mentioned in Sec. 2, the test sample shape (refer to Fig. 3) used in the stress measurement test was subjected to a stress analysis by the finite element method (FEM).

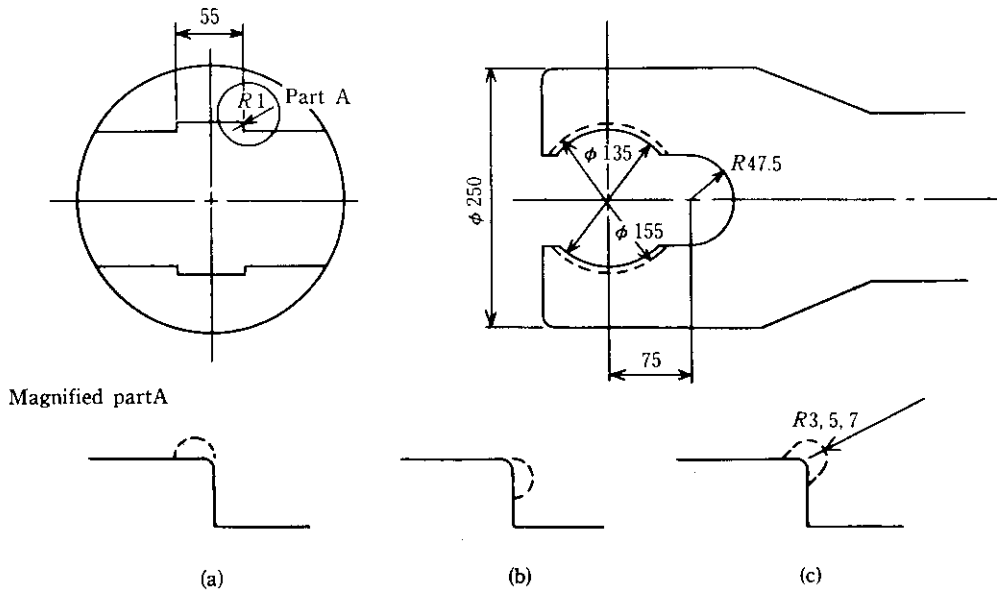


Fig. 3 Spindle head model for stress analysis using FEM and improvement ideas for the corner of slipper metal groove

Further, since increasing the corner radius of the slipper metal groove was effective as a measure for relieving stress concentration at the corner, a plan to improve the existing SJ, as shown by the broken line at the magnified part A in Fig. 3, was conceived. The FEM analysis was applied to model (c), which might be called a compromise between (a) and (b) in Fig. 3, and the corner radius of (c) was set at 3, 5, and 7 mm.

For the pressure distribution of the slipper metal which constitutes the load condition in the FEM analysis, the result³⁾ obtained by measurement with a prescale was used to enhance the analysis accuracy by approximating load conditions to actual ones. In performing the FEM analysis, first the entire model was analysed as shown in Fig. 4. To enhance the analysis accuracy, analysis was then applied to a zooming model in which only the slipper metal groove was given finer element division. Figure 5 shows the analysis results for the radius at the corner of the slipper metal groove, maximum stress, and the stress concentration factor.

Figure 5 indicates that an increase in the corner radius will lower the maximum stress and stress concentration factor. If the corner radius is increased to 7 mm or above, the maximum stress and stress concentration factor will further drop, but as was mentioned in Fig. 5, it is necessary to note that mean stress will increase.

From the above, the following findings were obtained:

- (1) Stress concentration factor α at the corner of the slipper metal groove is 2.8, when corner radius/outer diameter = $1/250 = 0.004$. Since the corner radius/outer diameter ratio in actual mills is within

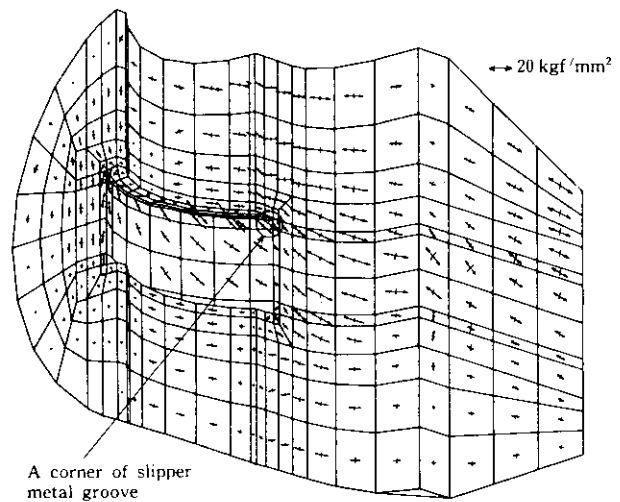


Fig. 4 Divided model for FEM and principal stress distribution of spindle head

the range of 0.0022 to 0.0061, the ratio of 0.004 may be said to represent a typical average value.

- (2) When the corner radius of the slipper metal groove is increased to

$$\text{corner radius/outer diameter} = 7/250 = 0.028,$$
 maximum stress drops from 39.9 kgf/mm^2 to 27.0 kgf/mm^2 , an increase in strength of about 1.5 times expected.
- (3) In the conventional SJ strength calculation method, stress concentration at the slipper metal groove is not taken into consideration. However, as shown by the results of the FEM analysis, the corner of the slipper metal groove receives maximum stress due

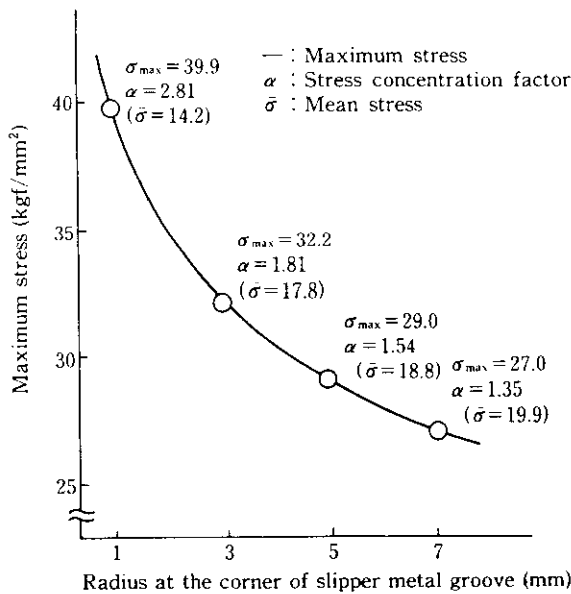


Fig. 5 Relation between radius at the corner of slipper metal groove and maximum stress

to stress concentration, and therefore, stress concentration should be taken into consideration in the future.

3.2 Conception of New SJ

If the corner radius of the slipper metal groove of the original SJ is increased, a certain degree of strength improvement can be expected, but it is insufficient because stress concentration has not been avoided. Here it is necessary to clarify the causes of generation of stress concentration, in order to prevent its occurrence and realize a spindle yoke shape of sufficient strength.

The cause of stress concentration generation is the application of load to the outside of the fillet, as shown in Fig. 6 (a). Because stress is concentrated on the fillet, it becomes a dangerous section. Further, considered in terms of the torsion of the bow-shaped section, maximum torsional stress occurs at the center of the chord of the bow.²⁾ Since the slipper metal groove lies at this maximum torsional stress generation position, its strength is lowered due to the decreased capability of the bow-shaped section. As can be seen in Fig. 4, the principal stress near the slipper metal groove is applied to the fillet in an oblique direction, causing stress concentration. Thus the original SJ inevitably has an intrinsic problem of strength drop owing to the characteristics of its shape.

Figure 6 (b)⁴⁾ shows the new SJ, which ingeniously avoids the above-mentioned intrinsic problem. In the new SJ, as can be seen from Fig. 6 (b), no load is applied to the outside of the fillet, thereby avoiding the effects of stress concentration. Further, the fillet was shifted to the outer diameter side, away from the position of maximum torsional stress generation. Since the fillet and main stress run in parallel directions, there is no risk of the occurrence of stress concentration. As mentioned above, the new SJ has completely eliminated the central problem with the original SJ and points toward significant improvements in strength.

4 Strength of Roll Coupling

To calculate the strength of the roll coupling shown in Fig. 7, the Okubo's method⁵⁾ can be used. In this method, the strength is obtained by torsion of the oval-shaped section. However, since this method uses data in which $B/D = 0.5$ to 0.875 , it cannot be applied to an

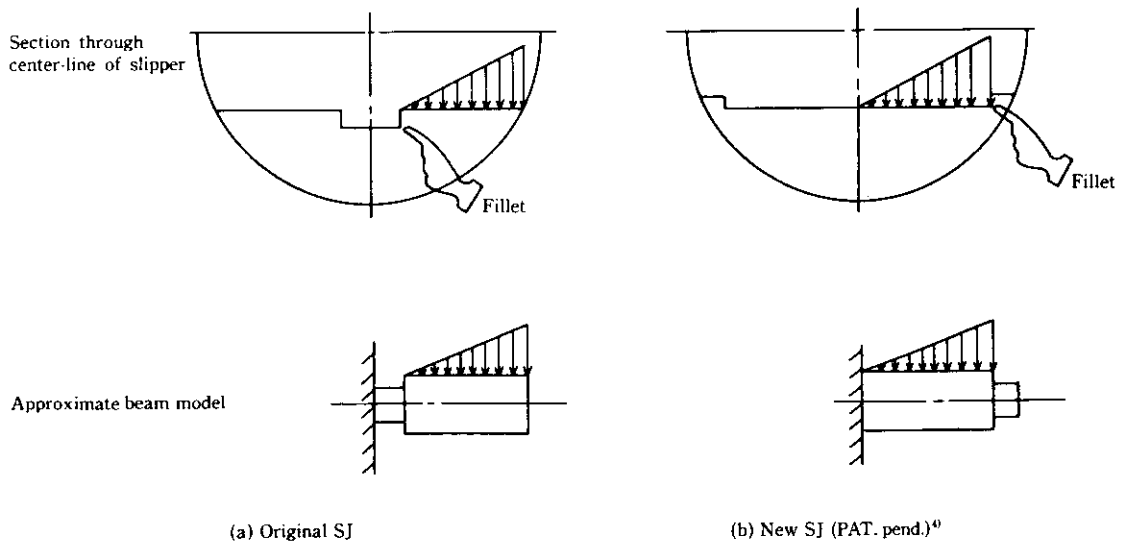


Fig. 6 Approximate beam model in the section of SJ through center-line of slipper

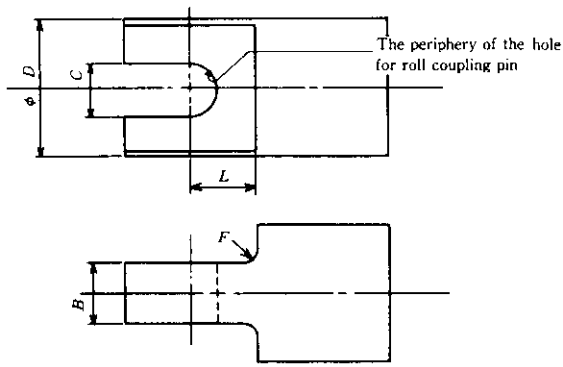


Fig. 7 Roll coupling

actual roll coupling where $B/D = 0.28$ to 0.34 is applicable. Therefore, a rectangular section method^{6,7)} is used in which the ovalshaped section is approximated to an equivalent rectangular section. According to this rectangular section method, torsional stress is obtained by Eq. (1) within the actual dimensional range.

$$\tau = \frac{1}{0.271} \times \frac{T}{D_1 B^2} \dots \dots \dots (1)$$

where

- T : Loading torque (kgf · mm)
- D : Dimension obtained by converting outside diameter D into equivalent rectangular longer side (mm)
- B : Fork thickness of roll coupling (mm)

However, the root of the fork has a fillet and is affected by stress concentration. The calculation methods for obtaining this stress concentration factor include a method using a round spindle having a fillet⁸⁾ and a method which employs a round spindle with a local plane on one side.⁹⁾ Both these methods, however, are approximate ones, and the stress concentration factors

obtained by the respective methods differ greatly. Further, there is no means of obtaining stress for the periphery of the hole for the roll coupling pin. Finally, there is no analysis method which takes into consideration the combination conditions of the roll coupling and spindle yoke.

For this reason, an FEM analysis was made of the shape shown in Fig. 8. Since stress at the fork root is considered to be governed by fork thickness B , corner radius of the fork root F , and length from slipper center line to root surface of roll coupling L , effects of these

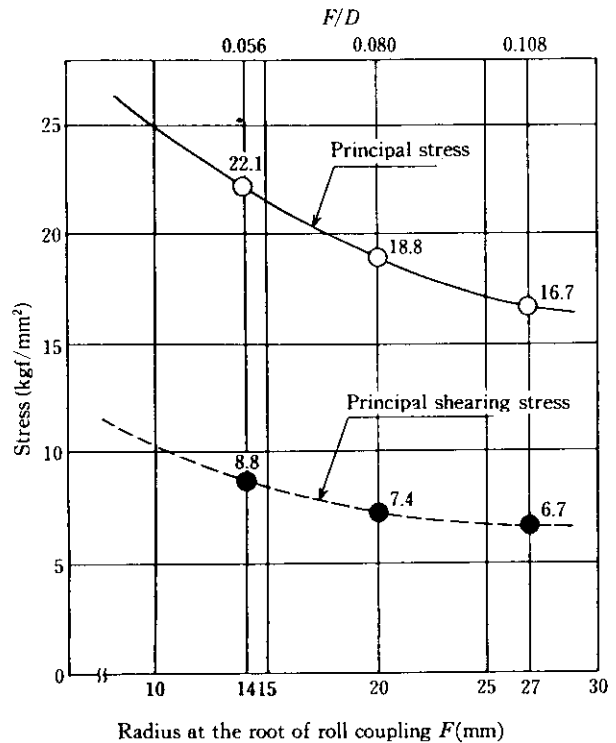


Fig. 9 Relation between radius at the root of roll coupling and stress ($B = 77.5$ mm, $L = 65$ mm)

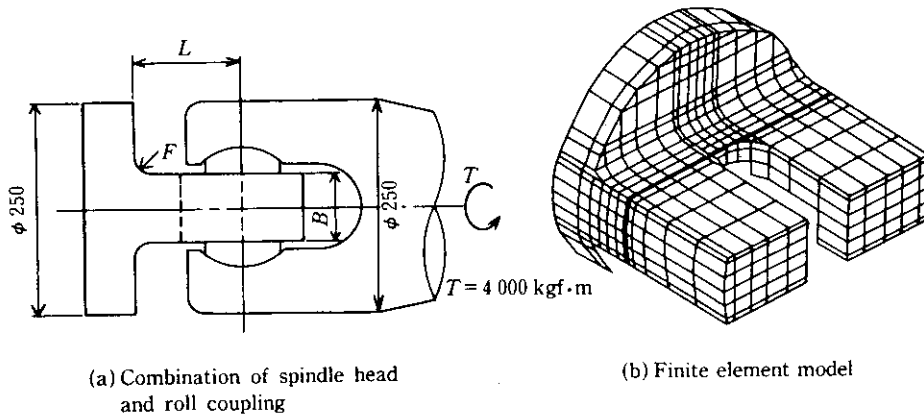


Fig. 8 Roll coupling model

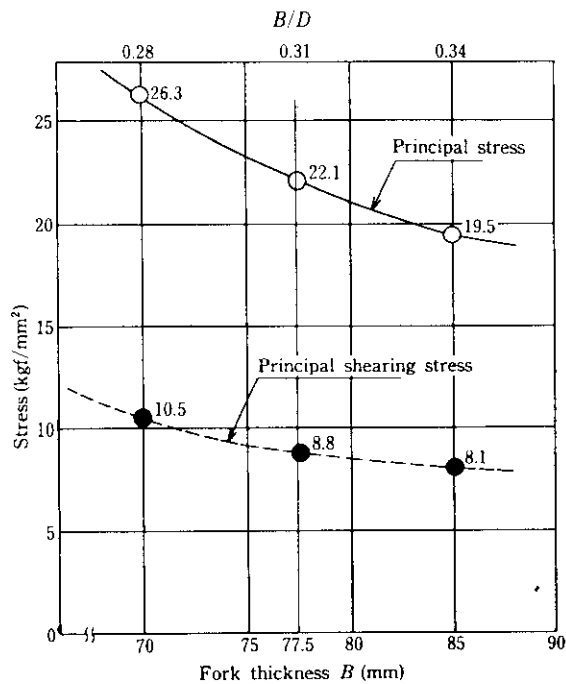


Fig. 10 Relation between fork thickness and stress ($F = 14$ mm, $L = 65$ mm)

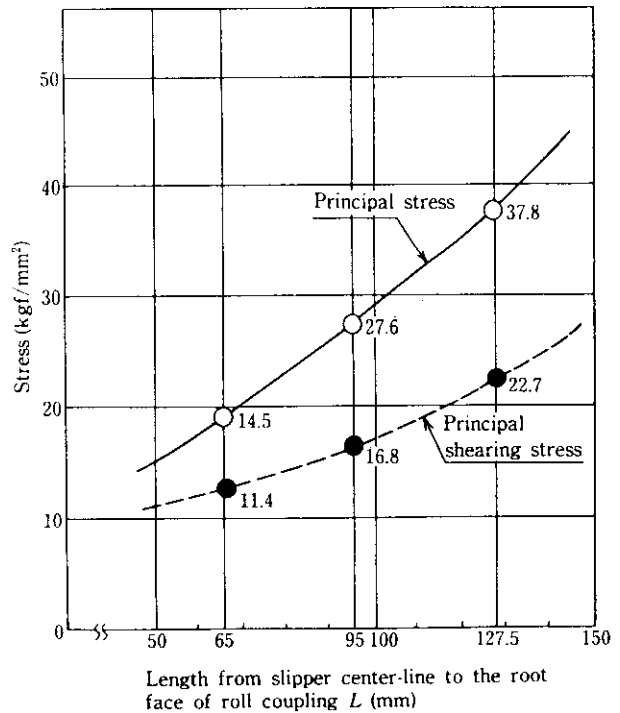


Fig. 11 Relation between length from slipper center-line to the root face of roll coupling and stress ($B = 70$ mm, $F = 20$ mm)

factors were investigated. The results are shown in Figs. 9, 10, and 11, where it is observed that effects on stress of fork thickness B , fork root corner radius F , and load acting point distance L , are great, and it has been confirmed that the stress level of the roll coupling is lower than that of the spindle yoke.

6 tf · m, taking into consideration the size of the experimental SJ. After verifying the linearity of the measured values, 4 tf · m was used as a standard in evaluating stress and strength.

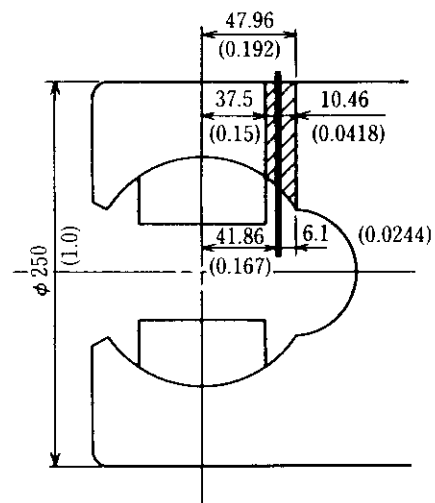
5 Stress Measurement Test

In obtaining accurate maximum stress at the spindle yoke and roll coupling, there is no better method than FEM analysis, but this method requires a considerable amount of work. For this reason, the authors made stress measurements on an experimental SJ with a strain gauge in order to verify the results of examinations so far made and to derive simplified experimental equations for maximum stress.

5.1 Dimensions of Experimental SJ and Loading Torque

The authors investigated the sizes of all SJ's in use at Mizushima Works and examined test specimen sizes and their combinations to find the effects of the corner radius of slipper metal groove r , the corner radius of fork root F , and the load acting point distance L . The results are shown in Table 1. The outside diameter of the experimental SJ was set at 250 mm.

To obtain load torque, stress at various parts of the experimental SJ was measured at the three levels of 2, 4,

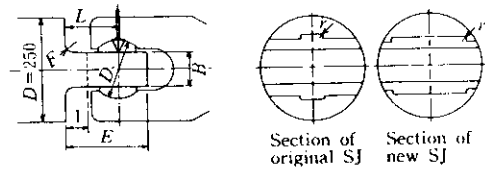


Dimensionless size is shown in ().
 //// : Lowest strength portion by material mechanics
 — : Center of the divided element in FEM

Fig. 12 Objective section in experiment

Table 1 SJ size experiment and combination of experimental condition

Experiment No.	SJ size						Length from slipper center-line to the root face of roll coupling					
	Spindle yoke			Roll-coupling			Case 1		Case 2		Case 3	
	Type	D_s	r	B	F	E	L	l	L	l	L	l
1	Original SJ	135	1	70	20	160	95	40	127.5	40		
2	"	135	5, 7	70	14	145	85	60	107.5	60		
3	"	135	1	85	30	150	95	70	112.5	70	127.5	70
4	"	135	5, 7	77.5	27	125	85	45	87.5	45	102.5	45
5	New SJ	110	3.4	70	20	135	95	40	97.5	40		
6	"	122.5	3.4	77.5	21	110	85	45	72.5	45		



5.2 Locations for Stress Measurements

Locations for stress measurements were selected on the basis of the results of examination by material mechanics and FEM analyses (refer to Fig. 12). However, since an SJ is complicated in shape, there is a possibility of overlooking maximum stress. For this reason, a brittle lacquer coating test was used to confirm stress distribution and principal stress direction of SJ, and based on closer understanding of stress characteristics, the location selection was made (refer to Fig. 13).

5.3 Results of Brittle Lacquer Coating Test

(1) Original SJ

As shown in Photo 1 (a), the original SJ developed a pattern of many cracks in its concave area. Cracks seemed to originate from the corner of the slipper metal groove. Further, the original SJ, in which the corner radius of the slipper metal groove had been enlarged to relieve stress concentration, developed a crack pattern similar to that shown in Photo 1 (b).

(2) New SJ

The generation of crack pattern as shown in Photo 2, indicates that crack density is lower than that in the original SJ, that cracks did not start from the corner radius, and that stress was dispersed. Compared with the original SJ, the new SJ was found to be free of stress concentration and low in stress, though

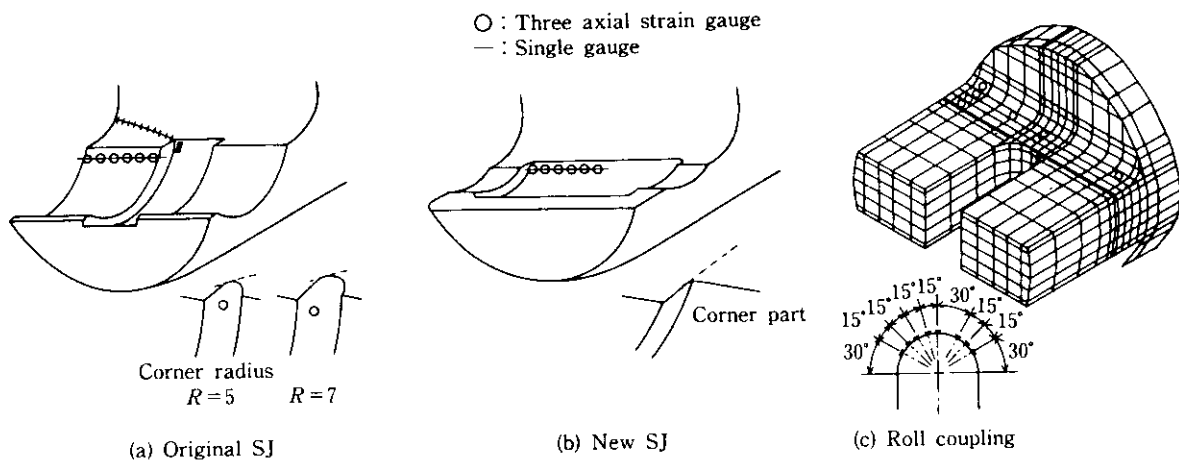


Fig. 13 Strain gauge location for stress measurement

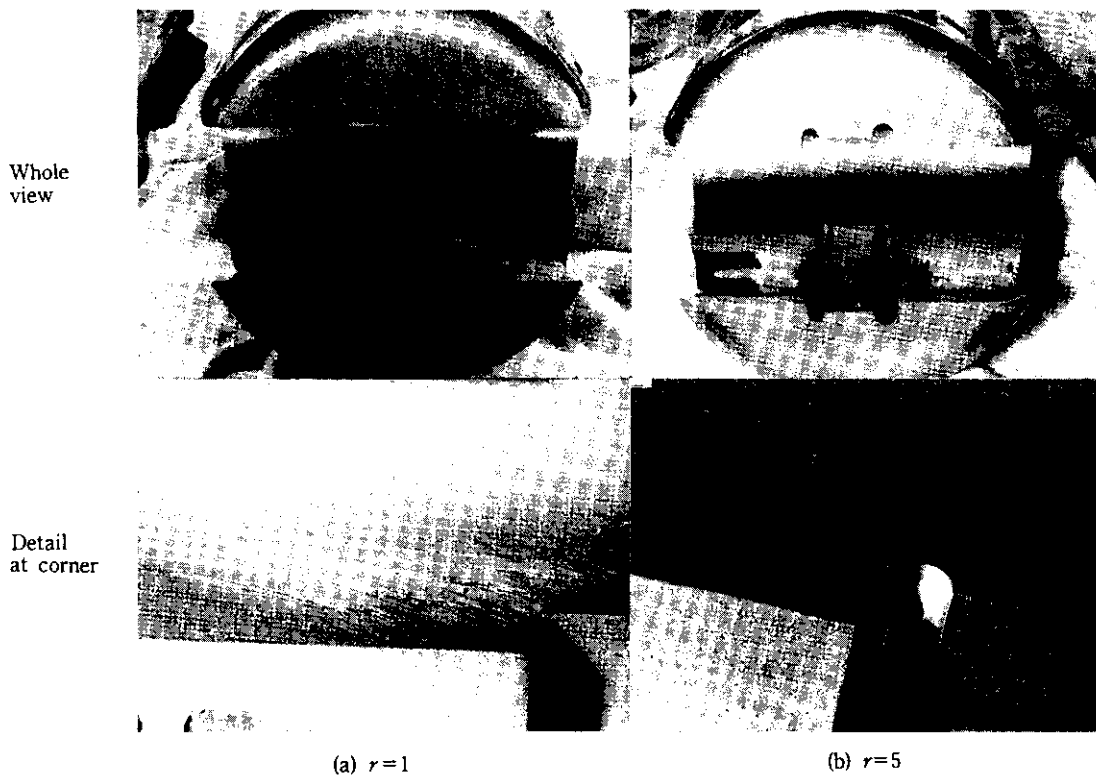


Photo 1 Brittle lacquer coating test at the concave and corner of slipper metal groove of original SJ

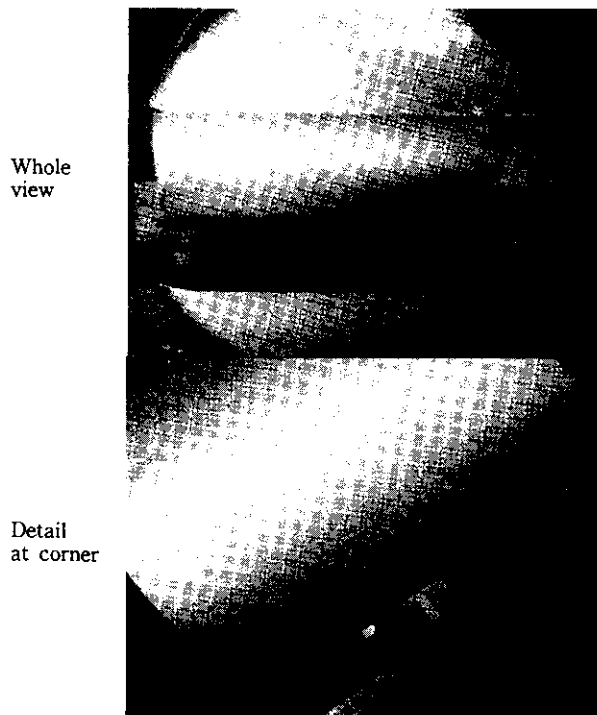


Photo 2 Brittle lacquer coating test results at the concave and corner of slipper metal groove of New SJ ($r = 3, 4$)

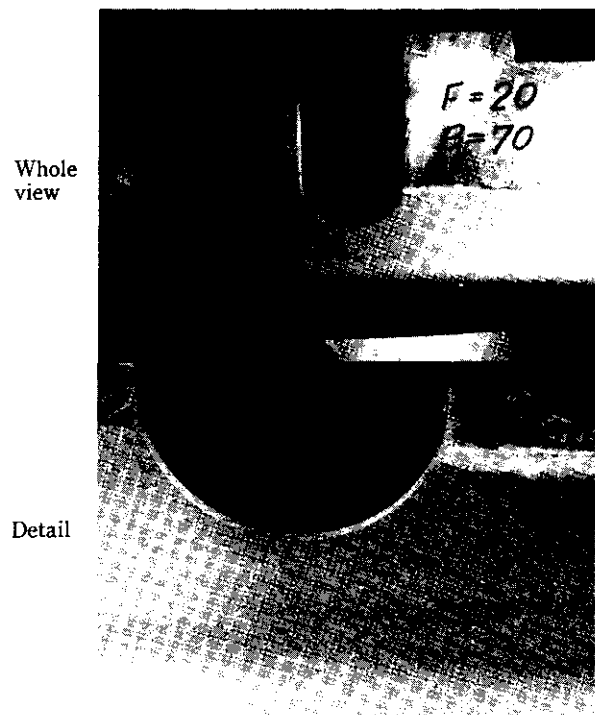


Photo 3 Brittle lacquer coating test result at the root of fork and the periphery of the hole for roll coupling pin

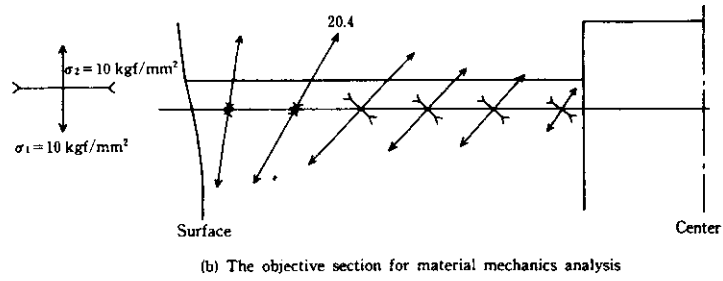
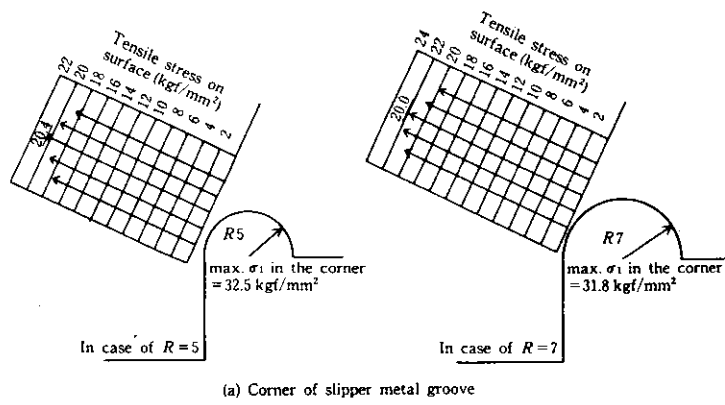


Fig. 14 Measured stress of original SJ ($D_s = 135$)

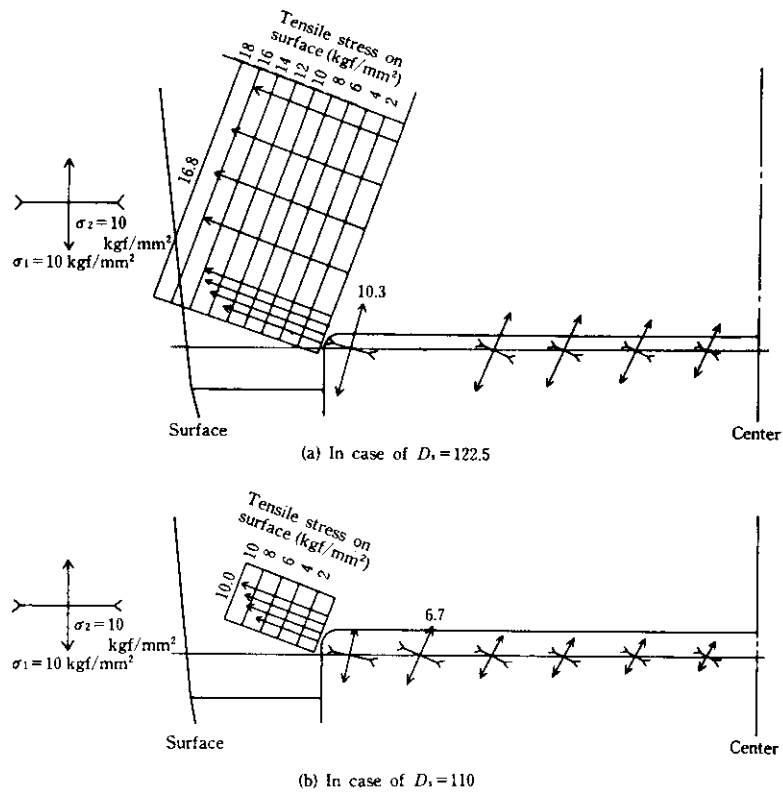


Fig. 15 Measured stress of new SJ at the objective section for material mechanics analysis and the corner of slipper metal groove

only qualitatively. The corner of the slipper metal groove does not form a dangerous section and can be said to have high strength.

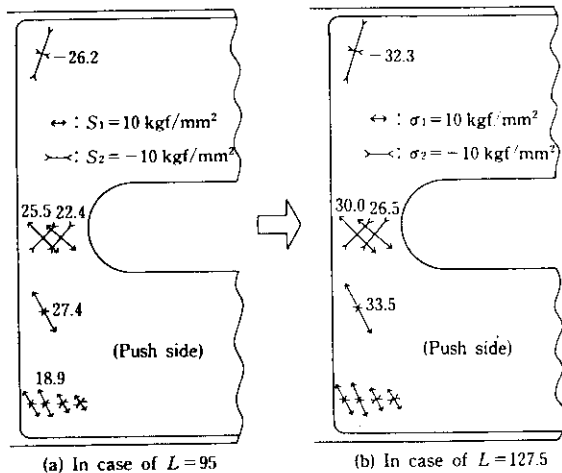
(3) Roll Coupling

As shown in Photo 3, the roll coupling developed crack patterns at the fork root and pin hole periphery, indicating high stress. The right half portion of the bottom photo in Photo 3 shows a crack pattern generated by tensile stress, and the left half portion shows a crack pattern generated by compressive stress, the two patterns crossing each other diagonally.

5.4 Results of Stress Measurements

Figures 14 and 15 show examples of measurement results of the original and new SJ, respectively; Figs. 16 and 17 show those of roll couplings.

The results of these stress measurements indicate the following:



(L: Length from slipper center-line to the root face of roll coupling)

Fig. 16 Measured stress of roll coupling ($B = 70$, $F = 20$, $E = 160$, $l = 40$)

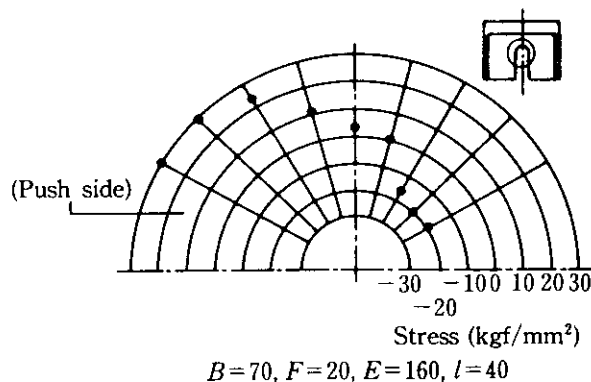


Fig. 17 Measured stress at the periphery of the hole for roll coupling pin

(1) Stress at Corner of Slipper Metal Groove of Spindle Yoke

Stress at the corner of the slipper metal groove is about 20 kgf/mm² for the original SJ (refer to Fig. 14 (a)) and about 14 kgf/mm² for the new SJ (refer to Fig. 15(a)), indicating lower stress with the new SJ.

At the concave portion of the slipper metal groove corner where fatigue cracks occurred in the past, even the original SJ whose corner radius was increased to relieve stress concentration still showed a high stress of about 32 kgf/mm² (refer to Fig. 14(a)), the same result as with the FEM analysis.

(2) Stress at Cross Sections Examined by Material Mechanics Analysis

In the original SJ, stress is low near the center, but becomes high near the outer diameter (refer to Fig. 14). In the new SJ, stress is slightly higher near the outer diameter than near the center, but not as high as with the original SJ (refer to Fig. 15). For outer diameter stress,

$$\text{new SJ} \ll \text{original SJ}$$

that is, the new design is highly effective in lowering stress near the outer diameter.

(3) Stress at Roll Coupling

As can be seen in Figs. 16 (a) and 17, maximum stress occurs near the fork root and around the pin hole, and these two stress values are nearly equal. The comparison between Figs. 16 (a) and (b) indicates that as the load acting point distance L increases, stress at the fork root increases.

6 Discussion

6.1 Stress Distribution and Maximum Stress at Spindle Yoke

(1) Comparison between Stress Measured and Calculated by Material Mechanics Analysis

Figure 18 shows the comparison between measured stress and stress calculated by Watanabe's method²⁾ at the section given a material mechanics analysis as indicated by the solid block line in Fig. 12. The figure indicates that in the new SJ,

material mechanics stress > measured stress is valid; that is, evaluation by material mechanics gives a higher stress value than the actual, causing underestimation of stress. For the original SJ, on the other hand,

material mechanics stress < measured stress is valid; evaluation by a material mechanics analysis gives a lower stress value than the actual, leading to an over-estimation of strength.

(2) Stress Distribution Characteristics of New and Original SJs

Stress distribution characteristics are described for

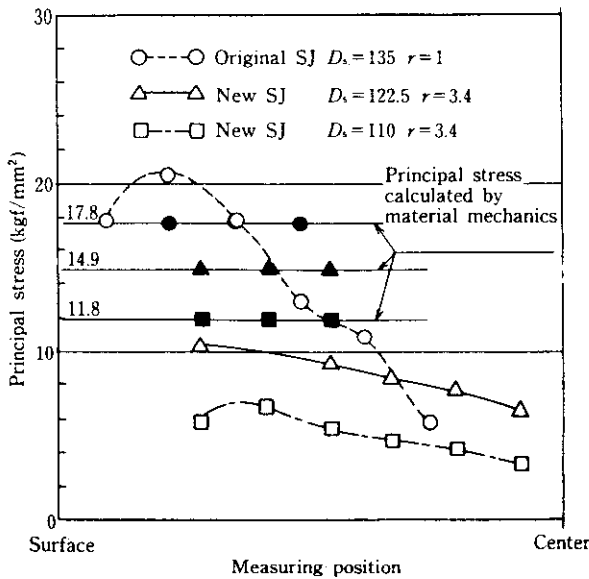


Fig. 18 Measured stress at the objective section for material mechanics analysis

the section subjected to material mechanics analysis, excluding the corner of the slipper metal groove where maximum stress is generated and fatigue cracks occur. As can be seen in Fig. 18, the stress distribution of the new SJ is a gentle slope with no local stress, while the original SJ shows a sharp slope and generation of local stress. These results indicate that the maximum measured stress for the original SJ is higher than in the new SJ, and that higher strength is obtained with the latter.

(3) Experimental Equations to Obtain Maximum Stress at New and Original Spindle Yokes

A comparison was made of measurement results of maximum stress near the slipper metal groove of the new and original SJ. Stress was calculated by a material mechanics analysis,²⁾ and experimental equations (2) and (3) for obtaining maximum stress were derived. Here the maximum stress at the slipper metal groove in the original SJ has been taken as "corner radius/outer diameter = 1/250," because this value is typical of the original SJ, as discussed above in item (1) of Sec. 3.1. Incidentally, the experimental level when the corner radius is changed in the original SJ is rare; hence this level has been excluded from the factors of experimental equation.

$$\text{New SJ: } \sigma_{\max(SJ)} = 340 \times D_s^{2.29} \times \frac{T}{D^3} \dots (2)$$

$$\text{Original SJ: } \sigma_{\max(SJ)} = 680 \times D_s^{2.29} \times \frac{T}{D^3} \dots (3)$$

where

- $\sigma_{\max(SJ)}$: Maximum principal stress of spindle yoke (kgf/mm²)
- D_s' : Dimensionless value of yoke diameter (D_s/D)
- T : Loading torque (kgf · mm)
- D : SJ outer diameter (mm)
- D_s : Yoke diameter (mm)

The error between values calculated by Eqs. (2) and (3) and measured values was within the range of -1.5 to +2.7%.

6.2 Stress Distribution and Maximum Stress of Roll Coupling

(1) Roll coupling pin hole shape

Since maximum stress near the fork root is nearly equal to that around the pin hole, the pin hole shape requires careful attention. The fork pin hole shape of the type shown in Fig. 19 (a) is considered better than that of the type shown in Fig. 19 (b).

(2) Comparison between FEM stress and measured stress in roll coupling

Figure 20 shows an example of a comparison between FEM stress and measured stress. The figure indicates that the two stress distributions show a fairly good agreement, with maximum stress values showing a good agreement. Therefore, if test data are analyzed and experimental equations are derived, they may be used as universal-purpose equations, eliminating the need to perform an FEM analysis in each case.

(3) Experimental equation to obtain maximum stress at roll coupling

Figures 16 and 17 show examples of measured results which correspond to experiment No. 1 in Table 1. Stress measurement results of experiment Nos. 2 to 6 have also been analyzed, and the experimental equation shown in Eq. (4) derived.

$$\begin{aligned} \sigma_{\max(\text{cplg.})} &= K \times \frac{(L' - 0.75F')^{0.5}}{B^{1.5} \times l^{0.84}} \times \frac{T}{D^3} \\ &= K \times \frac{(L - 0.75F)^{0.5}}{B^{1.5} \times l^{0.84}} \times \frac{T}{D^{1.16}} \dots (4) \end{aligned}$$

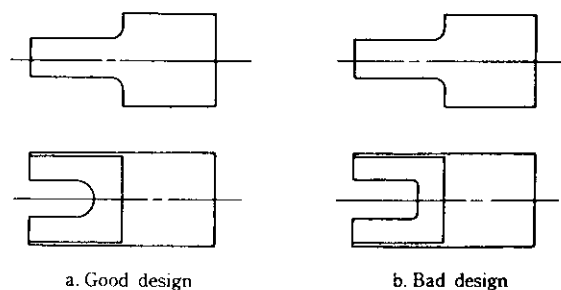


Fig. 19 Comparison of roll coupling design

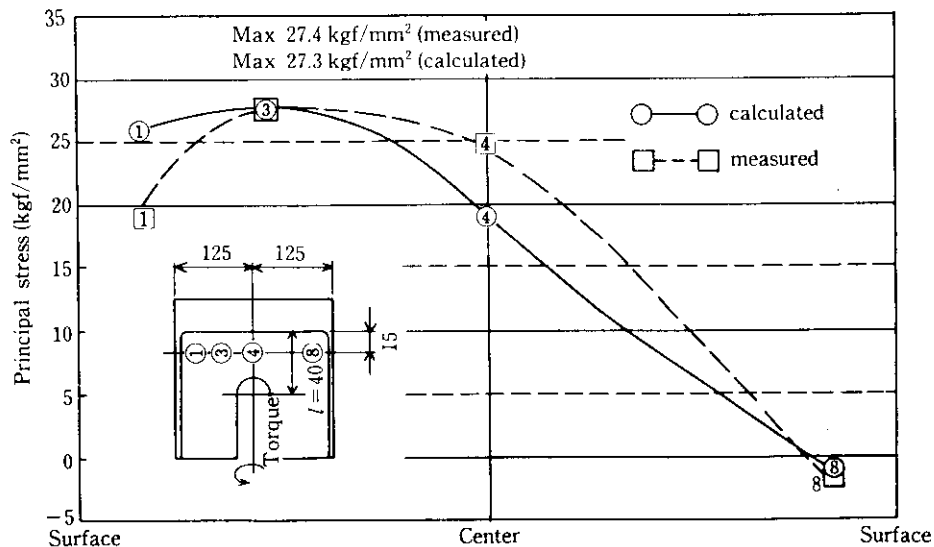


Fig. 20 Roll coupling stress measured, and calculated by FEM ($B = 70, F = 20, E = 160, L = 95, l = 40$)

where

$\sigma_{\max(\text{cplg.})}$: Maximum principal stress of roll coupling (kgf/mm^2)

K : Constant (6.81 for new SJ and 6.27 for original SJ)

L, F, B, l, D : Dimensions shown in attached figures of Table 1 in mm units; a prime mark (') indicates a dimensionless size value.

T : Load torque ($\text{kgf} \cdot \text{mm}$)

The error between values calculated by Eq. (4) and measured values was $\pm 8.4\%$. The FEM analysis stress at 100% of motor rating torque for the roll coupling in the plate mill at Mizushima Works was $47.8 \text{ kgf}/\text{mm}^2$, while the value calculated by Eq. (4) was $44.6 \text{ kgf}/\text{mm}^2$, thereby confirming that the error is within the above-mentioned range.

6.3 Strength Balance between Spindle Yoke and Roll Coupling

Figure 21 shows an example of the results of calculating the strength balance of a production rolling mill using Eqs. (2), (3), and (4). The figure indicates that spindle yoke stress \gg roll coupling stress for the original SJ. This is in good agreement with the fact that fracture occurs in the spindle yoke, but not in roll coupling. When the new SJ is used to correct this phenomenon, stress at the spindle yoke becomes lower than that of the roll coupling, and higher strength at the spindle yoke is realized.

7 Conclusions

To solve the problem of spindle yoke fracture occur-

ring frequently in recent years and to improve the strength of spindle yoke, a stress analysis and a study of the strength balance of the spindle yoke and roll coupling were carried out. The following results were obtained:

- (1) Through the improvement of the corner radius of the original SJ, stress at the slipper metal groove has been lowered and a slight strength improvement has become possible.
- (2) The new SJ is twice as strong as the original SJ, because it was so arranged that no load will act on the outside of the fillet of the slipper metal groove, thus avoiding the occurrence of stress concentration. Experimental equations have been derived for calculation of maximum stress.
- (3) Previously only torsional stress could be calculated for the roll coupling. An experimental equation for maximum stress, incorporating the shape and dimensional factors of the roll coupling, has now been derived.
- (4) A proposal has been made by the authors regarding the strength balance sheet for the spindle yoke and roll coupling.

Through the active use of the above-mentioned techniques, it is possible to achieve noticeable strength improvements in drive systems and prevent SJ fracture troubles. Thus these techniques can not only prevent the loss of production opportunity but also expand production capacity, thereby achieving a significant improvement in productivity.

References

- 1) K. Inoue: *The 57. 58th Nishiyama Memorial Seminar*, ISIJ, Tokyo, (1979), 255-257

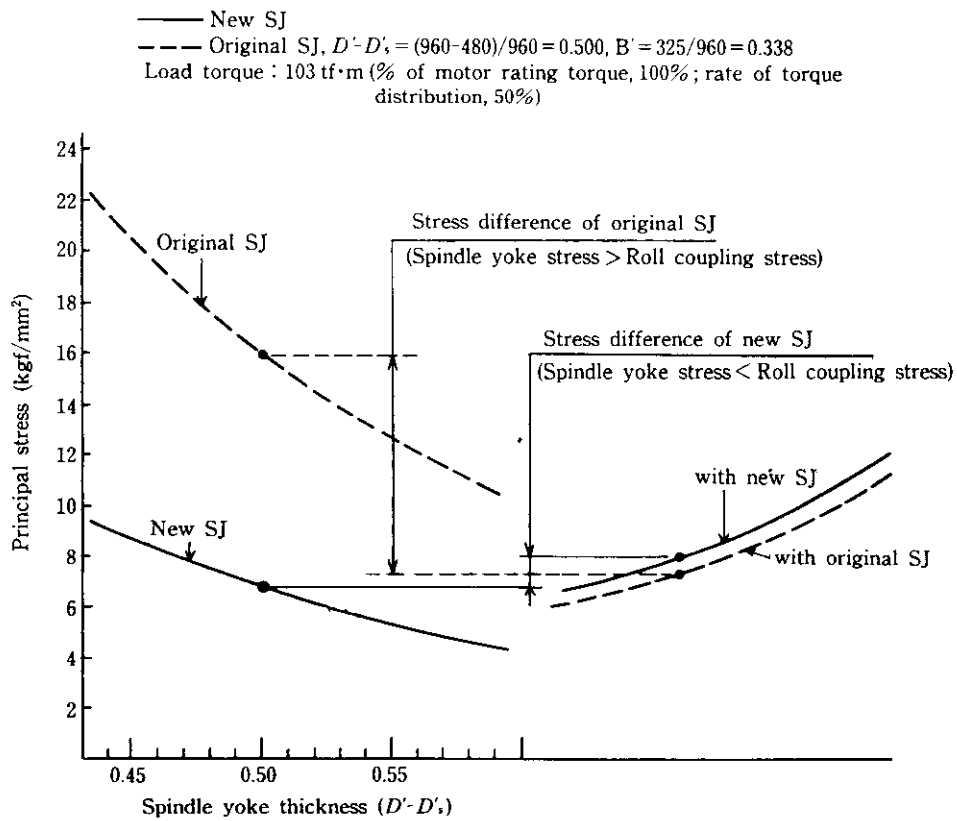


Fig. 21 Strength balancing sheet for hot strip rougher mill (R3 stand)

- 2) T. Watanabe: Preprint of Nihon Kikagakkai Ronbun, No. 140 (1965), 37-56, [JSME]
- 3) N. Inoue, F. Tanaka, H. Katayama, M. Ito, H. Kondo, K. Iijima: '82 Setsubi Kanri Zenkoku Taikai Text, (1982), B2-10, [JIPM]
- 4) Kawasaki Steel Corp.: Japanese Patent No. 59-80044, (1984)
- 5) "Kyodo Sekkei Databook", (1977), 615, [Syokabo]
- 6) "Kikaikogaku Binran (6)", (1977), 4-90 [JSME]
- 7) K. Yuasa: "Zairyo Rikigaku Koshikishu", (1980), 137-140, [Korona Sha]
- 8) M. Nishida: "Oryoku Shuchu", (1973), 646-647, [Morikita Shuppan]
- 9) H. Okubo: *Kikai no Kenkyu (Science of Machine)*, 25(1973)3, 421-424
- 10) Akira Kanno: *Haikan Gijyutsu (The Piping Engineering)*, 22(1980)8, 131-138